Original Article

Institution of MECHANICAL ENGINEERS
Journal of AEROSPACE ENGINEERING

Proc IMechE Part G:
J Aerospace Engineering
2015, Vol. 229(9) 1650–1660

DOI: 10.1177/0954410014558318
uk.sagepub.com/jaero
SAGE

Reynolds averaged Navier-Stokes simulations of compressible mixing layers of similar and dissimilar gases: Performance of *k*–ε turbulence model

Afroz Javed[1], NKS Rajan[2] and Debasis Chakraborty[1]

Abstract

The issue of growth rate reduction of high speed mixing layer with convective Mach number is examined for similar and dissimilar gases using Reynolds averaged Navier-Stokes (RANS) methodology with k–ε turbulence model. It is observed that the growth rate predicted using RANS simulations closely matches with that predicted using model free simulations. Velocity profiles do not depend on the modelled value of Pr_t and Sc_t; while the temperature and species mass fraction distributions depend heavily on them. Although basic k–ε turbulence model could not capture the reduced growth rate for the mixing layer formed between similar gases, it predicts very well the reduced growth rate for the mixing layer for the dissimilar gases. It appears that density ratio changes caused by temperature changes for the dissimilar gases have profound effect on the growth rate reduction.

Keywords

Compressible mixing layer, k–ε turbulence model, Reynolds averaged Navier-Stokes simulations

Date received: 1 April 2014; accepted: 13 October 2014

Introduction

In a scramjet engine, mixing of fuel and oxidizer takes place along the length of the combustor at very high speeds in a confined environment under compressible conditions. The understanding of compressible mixing layer becomes necessary to address the issues related with mixing and combustion in a scramjet engine. The rate of mixing is quantified by the growth rate of the thickness of mixing layer in downstream direction. This growth rate depends strongly on the ratio of the speeds of two mixing streams. The density ratio of the streams also affects the rate of mixing. A detailed expression to predict the mixing rate in an incompressible mixing layer depending on the velocity and density ratios was suggested by Dimotakis[1] and is given as $\left(\frac{\delta}{x}\right)_{\text{inc}} = \frac{C_\delta}{2}\frac{(1-r)(1+\sqrt{s})}{(1+r\sqrt{s})}\left[1-\frac{(1-\sqrt{s})/(1+\sqrt{s})}{1+2.9(1+r)/(1-r)}\right]$. In this expression *'r'* and *'s'* represent velocity and density ratios, respectively, C_δ is a proportionality constant with a value of 0.36, δ represents shear layer thickness at an axial distance of *'x'*. It has been observed through various experimental studies that with the onset of compressibility effects the Dimotakis'[1] expression for growth rates predicts higher values than those observed experimentally.[2–7] The compressibility effects are quantified using convective Mach number, M_c, defined as $\Delta U/(a_1 + a_2)$, with ΔU as the velocity difference between the two mixing streams and a_1 and a_2 are the speeds of sound in the two streams. Slessor et al.[8] have collected some of the salient experimental data for compressible mixing layers and normalized it with the incompressible growth rate expression given by Dimotakis[1] for the same velocity and density ratios. It is observed that higher the value of M_c higher the effect of compressibility on the growth rate ratio. It is also observed that the growth rate of a compressible shear layer reduces by a factor of 4–5 as convective Mach number increases to 0.8, moreover, above the value of 0.8 for convective Mach number the growth rate reaches an asymptotic value of roughly 0.2 of its

[1]Directorate of Computational Dynamics, Defence Research and Development Laboratory, Hyderabad, India
[2]Department of Aerospace Engineering, Indian Institute of Science, Bangalore, India

Corresponding author:
Debasis Chakraborty, Directorate of Computational Dynamics, Defence Research and Development Laboratory, Kanchanbagh P.O., Hyderabad 500058, India.
Email: debasis_cfd@drdl.drdo.in

incompressible counterpart. Dimotakis[9] has suggested the ratio of compressible to incompressible growth rate as $\frac{\delta'_c}{\delta'_{inc}} = f_\infty + (1 - f_\infty)e^{-aM_c^2}$ by considering experimental data set. An asymptotic value of $f_\infty = 0.2$ and $a = 3$ in the exponent is considered for the data set. The reduction in growth rate of a compressible mixing layer is also observed through numerical studies carried out using Direct Numerical Simulation (DNS),[10–13] and Large Eddy Simulation (LES) methodologies.[14,15] In contrast to DNS and LES, Reynolds Averaged Navier-Stokes (RANS) simulations do not have as much computational costs involved. But there is a need to model the unclosed terms arising due to averaging process. This modelling is done through different turbulence models. Though several turbulence models from zero equation models to Reynolds stress based models are used to model the turbulence in flow field, it has been observed that k–ε turbulence model remains the most popular one due to its robustness and computational economy as compared with higher order models. However, since 1972, it has been known that the application of classical k–ε turbulence model for free shear layers shows more spreading than actually occurs[16] at compressible convective Mach numbers. Since then, over the years, many modifications to the k–ε turbulence model have been suggested. Zeman[17] and Sarkar et al.[18] gave the concept of dilatational dissipation to modify eddy viscosity models. A study has been carried out by Barone et al.[19] for various turbulence models for the prediction of growth rate of compressible turbulent mixing layer. This study compares both k–ε and k–ω turbulence models with Zeman[17] Sarkar et al.,[18] and Wilcox[20] corrections for dilatational dissipation. The convective Mach number range is from 0 to 1.5. It was found that the k–ε model with Zeman[17] compressibility correction and k–ω model with Wilcox[20] compressibility correction gave the lowest average relative error for the convective Mach number range considered. A revised form of sonic eddy concept (yielding smaller length scales than the Kim's proposal) introduced by Aupoix[21] could show improved predictions of spreading rate of high speed mixing layer. Unknown boundary conditions (e.g. external turbulence level) were quoted as major difficulties for validation of models from experimental data. Heinz[22] has suggested a modification in a coefficient for turbulence viscosity in the k–ε model to cater for the compressibility effects based upon the concept of gradient Mach number given by Sarkar.[23] All these modifications are based on the analyses and studies carried out for the mixing of similar gases at nearly the same temperature. But, in a scramjet engine combustor, dissimilar gases (fuel and oxidizer) at different temperatures mix with each other. Numerical and experimental studies reported in published literature addressing non-reacting mixing of two dissimilar gases are not many compared to the studies carried out for the mixing of similar gases.

In the present work, RANS simulations with k–ε turbulence model are carried out to understand the performance of this turbulence model in prediction of growth rates of compressible mixing layers formed between two different gases at different temperatures.

Computational details

There are several experimental studies carried out to study the growth rate of compressible mixing layer involving mixing of dissimilar gases at different temperatures.[24–28] In these studies, the temperature difference between the two mixing streams is quite modest (static temperature ratios of around 2.5). An AGARD report AGARD-AR-345[29] discusses test cases for both incompressible and compressible mixing layers. These experimental studies contain detailed measurements of different flow parameters and turbulence statistics like intensity of fluctuations. However, these experimental data deal with the mixing of similar gases (air/air) at not very different temperatures. In order to simulate the effects of large temperature difference between mixing streams, an experimental study carried out by Erdos et al.[30] (first flow condition in Table 2), where a large temperature difference (102 K and 2436 K) exists between the two mixing streams of hydrogen and nitrogen. The mixing duct has a rectangular cross section with height to width ratio of 0.5. In the upper part of the duct, hydrogen gas at a temperature of 103 K is injected through a single manifold of two Ludweig tubes and in the lower part of the duct nitrogen gas at a temperature of 2436 K is supplied through an expansion tube, both the gases are at Mach numbers of 3.1 and 4.0, respectively. Measurements in the experiment are limited to wall pressures and heat flux. The choice of this experimental condition gives an opportunity to study the effect of large temperature difference on the mixing of two dissimilar gases with large molecular weights difference under compressible conditions.

Table 1. Combinations of Pr_t and Sc_t values for simulations.

No.	1	2	3	4	5	6	7	8	9
Pr_t	0.3	0.3	0.3	0.9	0.9	0.9	1.5	1.5	1.5
Sc_t	0.3	0.9	1.5	0.3	0.9	1.5	0.3	0.9	1.5

Table 2. Simulation matrix of high speed confined mixing layer.

No.	Location	Species	Velocity (m/s)	Temperature (K)	Pressure (Pa)	Mach No.	M_c	Remarks
1.	Primary	N_2	3807	2436	27,580	3.99	0.8	Erdos experiment
	Secondary	H_2	2389	103	27,580	3.09		
2	Primary	N_2	2887	2436	27,580	2.99	0.6	Dissimilar gases at various M_c s & temperatures
	Secondary	H_2	1819	103	27,580	2.35		
3	Primary	N_2	1925	2436	27,580	1.99	0.4	
	Secondary	H_2	1230	103	27,580	1.59		
4	Primary	N_2	1527	300	27,580	4.32	0.8	Similar gases with same temperature at different M_c
	Secondary	N_2	962	300	27,580	2.72		
5	Primary	N_2	1145	300	27,580	3.24	0.6	
	Secondary	N_2	721	300	27,580	2.04		
6	Primary	N_2	763	300	27,580	2.16	0.4	
	Secondary	N_2	481	300	27,580	1.36		

RANS simulations

A commercial software CFX TascFlow[31] has been used to perform the RANS simulations. Three dimensional RANS equations alongwith k–ε turbulence model suggested by Launder and Spalding[32] are solved using a second order spatially accurate scheme. The domain for present computations is shown in Figure 1. The domain extends 535.0 mm in stream-wise direction, 25.4 mm along the lateral direction and 0.2 mm in the span-wise direction. In lateral direction, 101 elements are used with appropriate clustering in mixing layer zone and wall boundary layers. The maximum grid spacing occurs away from boundary layer and mixing layer zones and is around 0.4 mm. The minimum grid spacing occurs at the centre line and near walls and is equal to around 0.003 mm. In axial direction, 300 elements are used with minimum grid spacing of 0.5 mm near the splitter plate and maximum grid spacing of 3.0 mm near the end of domain. The model free simulations of Javed et al.[33] have shown that the averaged flow field essentially remains two dimensional for the same geometry and flow conditions. A small thickness in span-wise direction is considered for the RANS simulations by providing two equally sized elements. Very fine clustered grids are used in the mixing layer zone and wall boundary regions. The surface pressure for both upper and lower walls for three different grids namely $101 \times 67 \times 2$, $300 \times 101 \times 2$ and $361 \times 167 \times 2$ are plotted in Figure 2. A very small difference between the surface pressures from the last two grids, namely $300 \times 101 \times 2$ and $361 \times 167 \times 2$ demonstrate the grid independence of the results.

Supersonic inlet condition is imposed for both hydrogen and nitrogen streams for the inlets. The velocity has been given as a profile boundary condition to cater for the boundary layer on the walls and splitter plate, with a parabolic boundary layer profile.

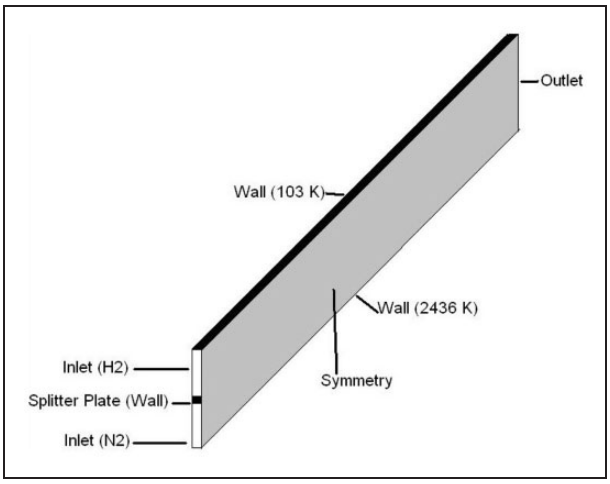

Figure 1. Computational domain with boundary conditions.

The inflow turbulence is specified as turbulence intensity $\left(\sqrt{\frac{2}{3}k}/V\right)$ of 0.01 and ratio of turbulent to molecular viscosity as unity. The walls are kept at constant temperature with hydrogen side wall at 103 K temperature and nitrogen side wall at 2436 K temperature. The two sides have been given symmetry boundary condition. Since the flow is supersonic throughout, the outlet boundary condition is considered as supersonic outlet. Turbulent diffusion of enthalpy and species are modelled using concept of turbulent Prandtl (Pr_t) and Schmidt (Sc_t) numbers. The values of these numbers considered for different simulations are listed in Table 1. The convergence criterion has been taken as the normalized residuals to be less than 1×10^{-5}.

It has been indicated by experimental measurements and DNS studies that Pr_t and Sc_t numbers for averaged flow fields can vary significantly in different regions of the flow even for relatively simple

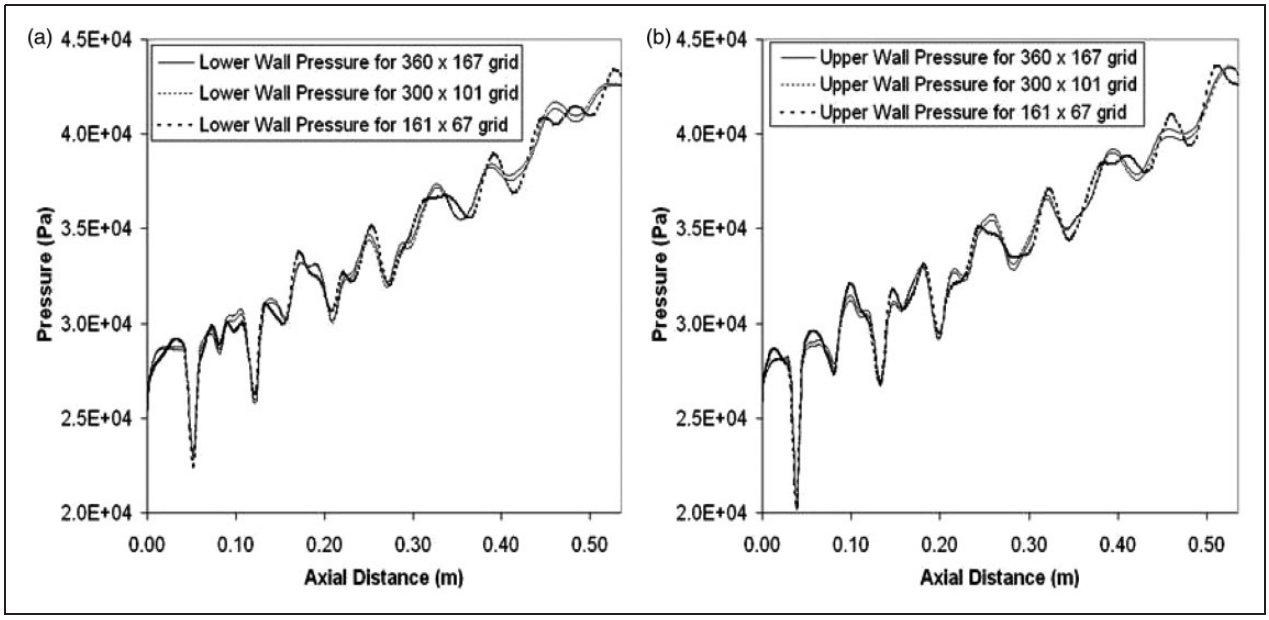

Figure 2. Surface pressure with three different grids (a) on lower wall and (b) on upper wall.

shear flows like boundary layers, jets and wakes etc.[34–37] A review on the turbulent Prandtl/Schmidt number in several free shear flows made by Reynolds[35] gives following variations (from core to outer region): round jet 0.73–1.7; round wake 0.8–0.3; plane jet 0.5–1.3; plane wake 0.5–0.7. In another review made by Baurle[37] for high speed reacting flows the range of turbulent Prandtl number variations for planar jets from 0.2 to 3.0, for round jets 0.7 to 2.0 and for backward facing step from 0.7 to 3.0. In the same review, the variation of the turbulent Schmidt number is found for planer jets from 0.1 to 2.2, for round jets from 0.1 to 2.0, for jet into cross flow from 0.1 to 0.5 and for injection behind a bluff body it is from 0.2 to 0.7. In these reviews, a large variation in the values of turbulent Prandtl and Schmidt numbers are shown. Also Baurle and Eklund[38] have used a variation from 0.25 to 1.8 to parametrically study flow field in a scramjet engine combustor. In the light of above it seems reasonable to study the present range of the values of Pr_t and Sc_t.

Model free simulations

A DNS can resolve the full range of physical scales of motion without need of any turbulence model, but its application is limited to flows with a relatively small Reynolds numbers. Higher Reynolds numbers are possible with LES, whose basic idea is to apply spatial filter(s) at a length scale Δ and include a subgrid model for the filtered stress terms, e.g. Smagorinsky model, to relegate the empiricism to just the smallest scales (although dynamic subgrid modelling shows promise in removing this as well). As Δ is decreased for a flow problem of given length scale, the subgrid model contribution is reduced and accuracy is increased. For some very high Reynolds number turbulent flows, if Δ is sufficiently reduced but is still greater than the Kolmogorov scale, the subgrid model influence becomes approximately negligible if the flow is not controlled by a laminar sublayer. Such flows include high Reynolds number turbulent free shear layers, jets, wakes and some sharp corner separated flow regimes for which further increases in Reynolds number do not significantly influence the bulk of the mean and turbulent field. Therefore, for a particular class of flows for which sufficient resolution is applied, one may simply neglect the filtering and the subgrid model stress terms and therefore eliminate any adjustable coefficients other than cell resolution. An extensive review of the model free simulation method and results for both non-reacting and reacting flows is provided by Givi.[39] This methodology of model free simulations has been used by many researchers and reported in literature. High resolution non-linear inviscid simulations were performed by Oh and Loth[40] for M_c values of 0.35, 0.45 and 0.7. The growth rate reduction with increasing M_c is well captured, the profiles of velocity and turbulence intensities match satisfactorily with the experimental observations of Goebel and Dutton.[41] Oh and Loth[40] carried out the study of the mixing layers in a 2D domain, 400 mm long and 47.6 mm wide to match experimental test set up size of Goebel and Dutton.[41] Euler equations were solved using the argument that viscous effect does not play a dominant role in the mixing layer region. The finest grid consisted of 20,000 points with a minimum grid spacing of 0.3 mm. Also it was reported that in order to achieve a good grid convergence the value of $\Delta x_{\min}/b$ should be equal to or lesser than 0.05 (for a second order numerical scheme[42]), where b is local shear layer thickness and $\Delta x_{\min}$ is the grid resolution. In another study involving the use of model free

simulations, Risha[43,44] considered a 3D domain of size $100\,\text{mm} \times 10\,\text{mm} \times 17\,\text{mm}$ and used a grid size of $100 \times 53 \times 35$ for studying free mixing layers formed between two air streams at different convective Mach numbers ($M_c = 0.2$–1.56) and obliquity angles. The model free simulations carried out by Chakraborty et al.[45] shows a good match of the wall pressures for the mixing study of the confined compressible mixing layer. The grid independence of the solution was demonstrated by not only comparing the mean values of the various thermochemical profiles with different grids but also higher order quantities. A good prediction of the different flow quantities in the compressible regime, by model free simulation technique makes it a suitable choice for the present study. Two different codes namely SPARK 2D and OpenFOAM are utilized to carry out the model free simulations. These codes and the simulations carried out are described briefly in the following sub sections.

SPARK 2D. Two dimensional model free simulations are carried out by employing non-reacting version of SPARK 2D code developed at the NASA LaRC by Drummond[46] and Carpenter.[47] It discretizes two dimensional Navier Stokes equations by using MacCormack's compact scheme with 4th order spatial and 2nd order temporal accuracy. This choice represents a compromise between the accuracy of higher order numerical algorithm and the robustness and efficiency of low order methods. This code has been validated by comparing the computed results of some test problems with known analytical solutions. Carpenter and Kamath[48] have demonstrated that with the compact scheme, the growth rate with the initial profile based on the Eigen functions predict those from linear stability theory for free shear layer to within 1% for a time duration equal to about five times the sweep time of the flow field. The compact scheme provide a substantial reduction in truncation and phase errors over the first order upwind and the second order MacCormack's scheme.

The numerical simulations are carried out for both the mixing of similar and dissimilar gases at different convective Mach numbers using SPARK 2D by Javed et al.[49] The details of flow parameters used in these simulations are shown in Table 2 for the sake of clarity.

OpenFOAM. OpenFOAM is free-to-use open source numerical simulation software with extensive CFD and multi-physics capabilities. The governing equations are discretized using polyhedral finite volume method. The object-orientation of the software facilitates easy model implementation in physical modelling and numerics (discretization, solvers, equation coupling). To the best of the knowledge of the authors, this may be the first attempt to apply OpenFOAM toolkit to solve high speed confined mixing layer. The governing equations are discretized to obtain a linear system of equations, which can be solved by the CFD solver. OpenFOAM has its own programming language for writing solution algorithms for complex physics. It includes set of functions that describe standard differential operators ($\nabla^2, \nabla\bullet, \nabla, \nabla\times, \partial/\partial t, \partial^2/\partial t^2$) which perform the discretization to create matrix equations. OpenFOAM offers different choice of methods for temporal discretization. For the discretization of the convective term, OpenFOAM offers many options. At runtime, the user can select the linear solver to be used to solve each matrix equation generated by a given application. The solvers are generalized so that the user can select the preconditioner and/or smoother for each solver. For the model free simulations in the present work temporal discretization is done using second order backward scheme. Fourth order schemes are used for spatial discretization. Preconditioned Bi-conjugate gradient solver (PBiCG) is used for the solution of velocity, enthalpy and species matrices with diagonal incomplete lower upper (DILU) preconditioner while preconditioned conjugate gradient (PCG) solver is used for pressure and density matrices with diagonal incomplete Cholesky (DIC) preconditioner. Pressure implicit with splitting of operators (PISOs) algorithm is used for the coupling between pressure and velocity terms with two corrector steps. A maximum Courant number of 0.3 is observed to give stable simulations.

Study of the Erdos experimental conditions has been made by Javed et al.[50] to analyse the effects of the side wall confinement. The mixing layer growth rates evaluated from these 3D simulations are used in the present work to compare the growth rates from RANS simulations.

Results and discussions

The axial velocity profiles for different combinations of Pr_t and Sc_t values are shown in Figure 3 which show that the choice of combination of Pr_t and Sc_t values do not affect the velocity profiles appreciably. All the velocity profiles lie within a band of less than 2% difference indicating that the values of Pr_t and Sc_t does not affect the shear layer growth rate for this particular case. The experimental condition considered for simulations has mixing of hydrogen at 103 K with nitrogen stream at 2436 K. Both the streams are having same static pressure. The density of hydrogen stream is 1.69 times more than that of nitrogen stream. The molecular mixing causes the molecular weight to be lesser than that of Nitrogen forcing the density to be lesser than nitrogen. However, the thermal mixing with such a large temperature difference, combined with the higher heat capacity of the hydrogen makes the gas mixture to have lower temperature than that of nitrogen stream and forces the density to be higher than that of the pure nitrogen stream. Due to these two opposing

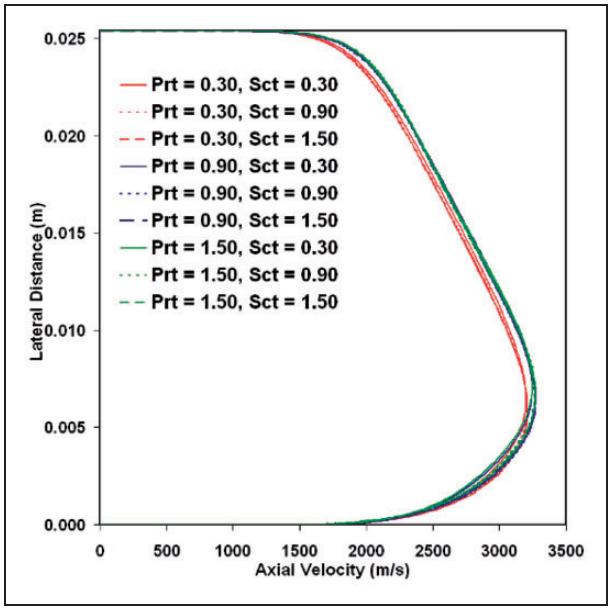

Figure 3. Axial velocity profiles in the lateral direction with different combinations of Pr_t and Sc_t values, at an axial location of 500 mm.

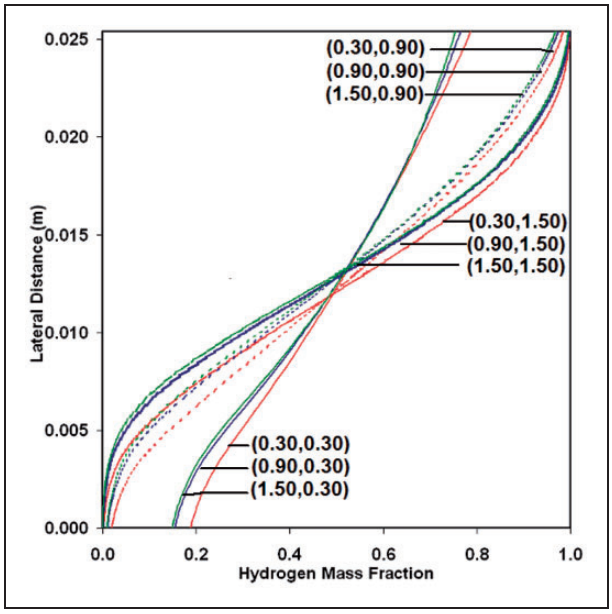

Figure 4. Hydrogen mass fraction profiles in the lateral direction with different combinations of Pr_t and Sc_t values, at an axial location of 500 mm. The values of (Pr_t, Sc_t) are shown next to the corresponding curve.

effects on the values of mean density the changes are not so drastic in the density field. When the values of Pr_t and Sc_t are varied, the changes introduced in the density field remain appreciably low to cause a large change in velocity field due to the counterbalancing effects of temperature and molecular weights of the mixing streams.

The distribution of hydrogen mass fraction in the lateral direction at the axial location of 500 mm is presented in Figure 4 with different values of Pr_t and Sc_t. The profiles are quite sensitive to the value of Sc_t while not so sensitive with the values of Pr_t. Also the same amount of change in the value of Sc_t does not cause the similar difference between the profiles, indicating a non-linear dependence of species mass fraction distribution on Sc_t values. This sensitivity of mass fraction distribution on Sc_t values makes the results from RANS simulations for the evaluation of mixing layer thickness based on species distribution, completely unreliable. Static temperature distributions in lateral direction with different values of Pr_t and Sc_t at an axial location of 500 mm shown in Figure 5 show its sensitivity to both the values of Pr_t and Sc_t. Hence both species distribution, temperature distribution prediction depends strongly on the choice of the values of Pr_t and Sc_t in RANS simulation; although velocity predictions are not affected by these values. For the prediction of an accurate distribution, a-priori knowledge of the suitable values of Pr_t and Sc_t for a similar kind of flow is necessary, or a suitable model for the evaluation of these parameters would be required.

The wall pressure comparisons with the experimental[25] values and RANS simulation are shown in Figure 6(a) and (b) for lower and upper walls

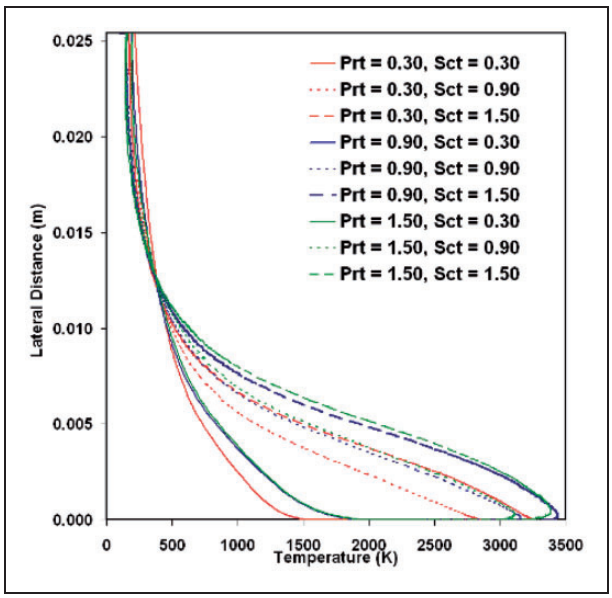

Figure 5. Static temperature profiles in the lateral direction with different combinations of Pr_t and Sc_t values, at an axial location of 500 mm.

respectively. Also in the same figures the wall pressure data from model free simulations[26] are plotted for the purpose of comparison. The waviness observed in the wall pressure data is due to reflections of multiple weak shocks and expansions waves from the walls. Except for some experimental points for lower wall, shown in Figure 6(a), RANS simulations overpredict the surface pressure. The surface pressures at upper wall are slightly under predicted by RANS simulations as shown in Figure 6(b). Nevertheless,

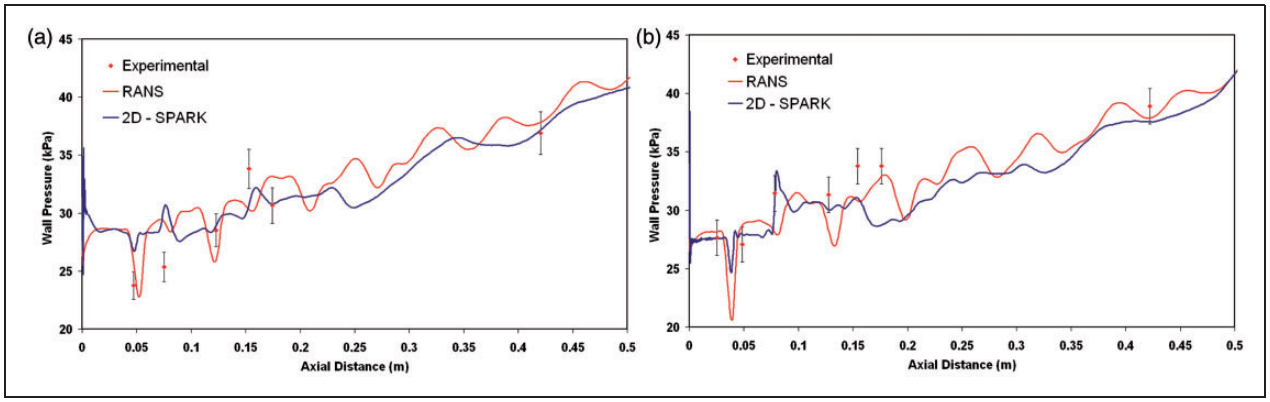

Figure 6. Wall pressure comparison from RANS and experimental results for (a) lower wall (nitrogen side) and (b) upper wall (hydrogen side).

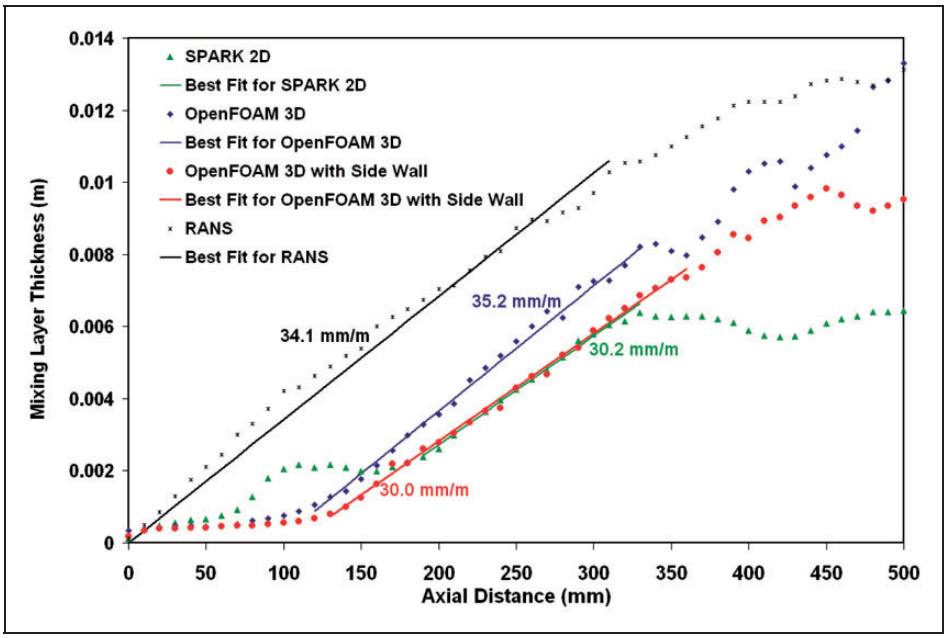

Figure 7. Mixing layer thicknesses and growth rate from RANS simulations, data from the model free simulations are also plotted for comparison.

considering the repeatability of the experiment the comparison can be considered as reasonably good. The surface pressures from RANS simulations also show a good match with that predicted from model free simulations using SPARK code.[26]

Vorticity thickness defined as $\delta_\omega = \Delta U \Big/ \left(\frac{\partial u}{\partial y}\right)_{\max}$ is used to evaluate the shear layer thickness. Here ΔU is the difference in velocities of the two mixing streams. The values of shear layer thicknesses for the present simulation along with the best fit in the linear region are shown in Figure 7. Shear layer thicknesses from the model free simulations carried out by Javed et al.[43] for 3D geometry with symmetry boundaries in the sides and with the actual side wall are also shown in the figure, which are evaluated using OpenFOAM software. The 2D simulation results shown in the Figure 7 are taken from the model free simulations carried out by Javed et al.[26] using SPARK 2D. The shear layer thicknesses at the same axial positions are different due to the different locations of attainment of self similarity for the different simulations. However, the slopes of the lines joining the thickness points, which represent growth rate of the mixing layer, are almost identical. In the downstream of the linear region, the thicknesses show a sudden decreasing trend for the 2D simulations and decreasing and increasing trend for 3D simulation. This kind of behaviour is shown due to the fact that as the shear layer grows, the shear layer profile may not remain perfectly linear in the lateral direction. With non linearity, the value of $(\partial u/\partial y)_{\max}$ at some points in the shear layer can be more, which remains almost constant in case of a linear profile. In such situation, even though the thickness is higher, this increased value of $(\partial u/\partial y)_{\max}$ (which occurs in the

denominator while evaluating vorticity thickness), returns a smaller value.

It can be observed that the growth rate predicted by the RANS simulation differs only slightly with the model free simulation growth rate predictions. This good match of the growth rate looks contrary to the findings[16] that the use of k–ε turbulence model is not suitable to predict the growth rates of compressible shear layers.

In order to further check the performance of k–ε turbulence model at different convective Mach numbers, number of simulations is performed. The different parameters for the simulation matrix are shown in Table 3. The temperatures, pressures and compositions of both the streams are kept same as that used in Erdos experimental condition.[25] This makes the density ratio for all the cases to be equal to 1.69.

Mixing layer simulations using RANS have also been made for mixing two supersonic streams at same temperature, pressure and composition at different values of M_c. For these simulations, a numerical study case carried out by Kral[51] has been chosen. In this study, mixing of two supersonic streams has been considered at 800 K static temperature. The flow Mach numbers of both the streams and corresponding M_c are given in Table 4.

The shear layer vorticity growth rate ratios, are the values of vorticity thickness growth rate of compressible shear layer normalized with the corresponding incompressible shear layer growth rates, are plotted in Figure 8. The incompressible shear layer growth rate is evaluated using Dimotakis'[1] relation which includes both velocity and density ratios. Apart from the results from the cases tabulated in Table 3 which are simulated using RANS simulations, the similar and dissimilar gases mixing cases result from model free simulations[42] along with Dimotakis'[9] curve are also shown by closed symbols. The model free simulations were carried out using SPARK 2D software, details of which are available in Oh and Loth.[42]

An examination of the similar gas cases in Figure 8 shows that the model free simulations capture the reduction in the growth rate matching well with the Dimotakis'[9] curve. It can be observed in the same figure that the RANS simulations for these cases show almost no sensitivity towards compressibility. Similar result has been obtained by Kral,[51] for simulation of free mixing layer with $M_c = 0.1$–4.0.

The growth rate ratios of dissimilar gases obtained using model free simulations show a higher growth rate when compared with the cases of similar gases

Table 3. Flow parameters for the mixing layer study in different cases.

Case	Location	Velocity (m/s)	Mach number	Velocity ratio (r)	M_c
1	Primary	3807	3.95	0.95	0.1
	Secondary	3629	4.69		
2	Primary	3807	3.95	0.91	0.2
	Secondary	3451	4.46		
3	Primary	3807	3.95	0.81	0.4
	Secondary	3095	4.00		
4	Primary	3807	3.95	0.72	0.6
	Secondary	2739	3.54		
5	Primary	3807	3.95	0.63	0.8
	Secondary	2383	3.08		
6	Primary	3807	3.95	0.53	1.0
	Secondary	2027	2.62		
7	Primary	3807	3.95	0.44	1.2
	Secondary	1670	2.16		
8	Primary	3807	3.95	0.35	1.4
	Secondary	1314	1.70		
9	Primary	3807	3.95	0.25	1.6
	Secondary	958	1.24		

Table 4. Flow parameters for the compressible mixing layer simulation with unity static temperature ratio.

M_c	0.1	0.5	1.0	1.5	2.0	2.5	3.0	3.5
M_1	1.6	2.4	3.4	4.4	5.4	6.4	7.4	9.4
M_2	1.4	1.4	1.4	1.4	1.4	1.4	1.4	1.4

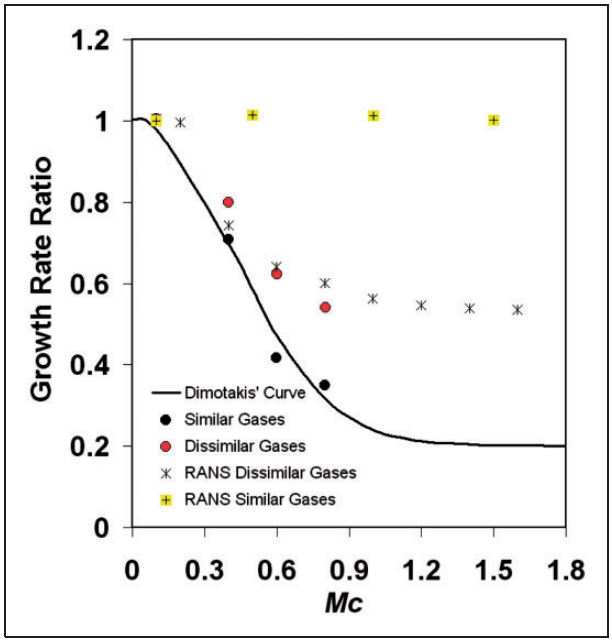

Figure 8. Variation of the ratio of compressible to incompressible growth rate for different simulations.

at the same convective Mach numbers. The higher growth rate occurs due to the dominant effect of temperature on the density as compared with that of pressure (compressibility effect). The cause for the higher growth rate of dissimilar gases mixing layers is discussed by Javed et al.[49] in detail.

The growth rate ratios predicted from RANS using k–ε turbulence model for dissimilar gases show a reduction in contrast with those predicted for similar gases at the same convective Mach numbers. This kind of reduction is also observed in the simulations carried by Viegas and Rubesin[52] using k–ε turbulence model for parallel compressible mixing of high static temperature ratio gas streams. In the simulations performed by Viegas and Rubesin,[52] both matched static temperatures as well as different static temperatures cases were considered. In the different static temperature cases, the total temperatures of both the streams were matched, and the static temperature ratios were varied from 1.45 to 33.33 for different M_c. For matched density case, the reduction in the growth rate at $M_c = 1.5$ was marginal (8%); while it was 45% at the same M_c for different density cases. The present simulations employ a static temperature ratio of 23.65. This reduction of growth rate could be due to change of density in the mixing layer due to dominant effect of temperature change in comparison of the effect of pressure as explained by Mahle et al.[53] and Javed et al.[49]

Further observation of Figure 8 shows a good match of growth rates predicted from both model free simulations as well as through RANS simulations using k–ε turbulence model. This good match can be attributed to the capturing of density change effects due to temperature by turbulence model, while the model is unable to capture density changes caused by pressure fluctuations as can be observed by the results of similar gases mixing at same temperature.

Conclusions

RANS simulation with k–ε turbulence model is performed to examine its adequacy for prediction of the growth rate of mixing layer formed between two dissimilar gases. It has been observed that the values of Pr_t and Sc_t do not affect velocity distribution, however, the temperature and species mass fraction distribution are strongly affected. The wall pressures evaluated exhibit a close match with both experimental as well as model free simulation results. Growth rate of shear layer is also observed to match closely with model free simulation results. In order to get an explanation for this close match, a number of similar and dissimilar gases compressible mixing simulations have been performed at different M_c values. It has been observed from Figure 8 that the growth rates reduction of dissimilar gases show a good match for both RANS and model free simulation. However, the growth rate of similar gases does not show any sensitivity towards increasing M_c when evaluated from RANS methodology. The reason for this behaviour is explained to be due to the dominant effect of temperature changes on density than that due to pressure. The reduction observed gives strong evidence that the growth rate decrease in case of compressible mixing of different gases at large temperature difference is governed by the effect of temperature on density rather than the effect of pressure (compressibility effect).

Conflict of interest

None declared.

Funding

This research received no specific grant from any funding agency in the public, commercial, or not-for-profit sectors.

References

1. Dimotakis PE. Two-dimensional shear-layer entrainment. *AIAA J* 1986; 24(11): 1791–1796.
2. Papamoschou D and Roshko A. The compressible turbulent shear layer: an experimental study. *J Fluid Mech* 1988; 197: 453–477.
3. Elliot GS and Samimy M. Compressiblity effects in free shear layers. *Phys Fluid A2* 1990; 7: 1231–1240.
4. Goebel SG, Dutton JC, Krier H, et al. Mean and turbulent velocity measurements of supersonic mixing layers. *Exp Fluids* 1990; 8: 263–272.
5. Goebel SG and Dutton JC. Velocity measurements of compressible turbulent mixing layers. *AIAA J* 1991; 29: 538–546.
6. Barre S, Quine C and Dussauge J. Compressiblity effects on the structure of supersonic mixing layers: experimental results. *J Fluid Mech* 1994; 259: 47–78.

7. Clemens NT and Mungal MG. Large-scale structure and entrainment in the supersonic turbulent mixing layer. *J Fluid Mech* 1995; 284: 171–216.
8. Slessor MD, Zhuang M and Dimotakis PE. Turbulent shear-layer mixing; growth-rate compressibility scaling. *J Fluid Mech* 2000; 414: 35–45.
9. Dimotakis PE. Turbulent free shear layer mixing and combustion. In: SNB Murthy and ET Curran (eds) *High speed flight propulsion system 1991, 137, progress in astronautics and aeronautics*. Reston: AIAA Publication, pp.265–340.
10. Elliot GS and Samimy M. Compressiblity effects in free shear layers. *Phys Fluids A2* 1990; 7: 1231–1240.
11. Vreman B, Sandham ND and Luo KH. Compressible mixing layer growth rate and turbulence characteristics. *J Fluid Mech* 1996; 320: 235–258.
12. Pantano C and Sarkar S. A study of compressibility effects in the high-speed turbulent shear layer using direct simulation. *J Fluid Mech* 2002; 451: 329–371.
13. Li Q and Fu S. Numerical simulation of high-speed planar mixing layer. *Comput Fluids* 2003; 32: 1357–1377.
14. Vreman B, Geurts B and Kuerten H. Large eddy simulation of the turbulent mixing layer. *J Fluid Mech* 1997; 339: 357–390.
15. Foysi H and Sarkar S. The compressible mixing layer: an LES study. *Theor Comput Fluid Dyn* 2010; 24: 565–588.
16. Launder BE, Morse A, Rodi W, et al. Prediction of free shear flows – a comparison of the performance of six turbulence models. *Free Turbulent Shear Flows* 1972; 1, NASA SP-321.
17. Zeman O. Dilatational dissipation – the concept and application in modelling compressible mixing layer. *Phys Fluids A2* 1990; 2: 178–188.
18. Sarkar S, Erlebacher G, Hussaini MY, et al. The analysis and modelling of dilatational terms in compressible turbulence. *J Fluid Mech* 1991; 227: 473–493.
19. Barone MF, Oberkampf WL and Blottner FG. Validation case study: prediction of compressible turbulent mixing layer growth rate. *AIAA J* 2006; 44(7): 1488–1497.
20. Wilcox DC. Dilatation-dissipation corrections for advanced turbulence models. *AIAA J* 1992; 30(11): 2639–2646.
21. Aupoix B. Modelling of compressibility effects in mixing layers. *J Turbulence* 2004; 5(No. N7).
22. Heinz S. A model for the reduction of the turbulent energy redistribution by compressibility. *Phys Fluids* 2003; 15(11): 3580–3583.
23. Sarkar S. The stabilising effect of compressibility in turbulent shear flow. *J Fluid Mech* 1995; 282: 163–186.
24. Wantuck PJ, Tennant RA, Rothstein AD, et al. *An experimental investigation of the properties of a non-reacting, supersonic shear layer*, 1991, AIAA Paper No. 91-0628.
25. Hall JL, Dimotakis PE and Rosemann H. *Experiments in non-reacting compressible shear layers*, 1991, AIAA Paper No. 91-0629.
26. Papamoschou D and Roshko A. The compressible turbulent shear layer: an experimental study. *J Fluid Mech* 1988; 197: 453–477.
27. Rossmann T, Mungal MG and Hanson RK. *An experimental investigation of high compressibility non-reacting mixing layers*, 2000, AIAA Paper No. 2000-0663.
28. Urban WD, Watanbe S and Mungal MG. *Velocity fields of the planar shear layer: compressibility effects*, 1998, AIAA Paper No. 98-0697.
29. AGARD-AR-345-A selection of test cases for the validation of large-eddy simulations of turbulent flows. January 1998, NASA-19980201044.
30. Erdos J, Tamagno J, Bakos R, et al. *Experiments on shear layer mixing at hypervelocity conditions*. 1992, AIAA Paper 92-0628.
31. CFX-TASC flow Computational Fluid Dynamics Software, Version 2.11.1, AEA Technology Engineering Software Ltd., 2001.
32. Launder BE and Spalding DB. The numerical computation of turbulent flows. *Comp Meth Appl Mech Eng* 1974; 3: 269–289.
33. Javed A, Chakraborty D and Paul PJ. Model-free simulations for compressible mixing layer. *J Aerospace Eng* 2013; 227: 977–991.
34. Launder BE. Heat and mass transport. In: P Bradshaw (ed.) *Turbulence 1976*, vol. 12 of Topics in Applied Physics. Berlin Heidelberg: Springer, pp.232–287.
35. Reynolds AJ. The variation of turbulent Prandtl and Schmidt numbers in wakes and jets. *Int J Heat Mass Transfer* 1976; 19: 757–764.
36. Kays WM. Turbulent Prandtl number – where are we? *ASME J Heat Transfer* 1994; 116: 284–295.
37. Baurle RA. *Modelling of high speed reacting flows: established practices and future challenges*, 2004, AIAA paper No. 2004-0267.
38. Baurle RA and Eklund DR. *Analysis of dual-mode hydrocarbon scramjet operation at Mach 4-6.5*, 2001, AIAA paper No. 2001-3299.
39. Givi P. Model Free Simulations of turbulent reactive flows. *Prog Energy Combust Sci* 1989; 15: 1–107.
40. Oh CK and Loth E. *A numerical investigation of supersonic turbulent shear layers: compressibility effects,* 1994, AIAA Paper No. 94-2244.
41. Goebel SG and Dutton JC. *Velocity measurement of compressible, turbulent mixing layers,* 1990, AIAA paper 90-0709.
42. Oh CK and Loth E. Effects of initial conditions on spatially evolving compressible shear layer simulations. *Comput Fluid Dyn* 1996; 6: 307–319.
43. Risha DJ. *Analysis of growth rates in three-dimensional air-to-air, supersonic shear layers using direct numerical simulation,* 1995, AIAA paper No. 95-0523.
44. Risha DJ. *Analysis of turbulence statistics in three-dimensional, air-to-air supersonic shear layers using direct numerical simulation,* 1995, AIAA paper No. 95-6072.
45. Chakraborty D, Mukunda HS and Paul PJ. Two dimensional direct numerical simulation of nonreacting confined supersonic mixing layer. *Aeronaut J* 2000; June): 291–296.
46. Drummond JP. Supersonic reacting internal flow field, in numerical approaches in combustion modeling. In: ES Oran and JP Borris (eds) *Progress in Aeronautics and Astronautics*. vol. 135: 1991, pp.365–420AIAA.
47. Carpenter MH. *A generalized chemistry version of SPARK*, 1998, NASA-CR-4196.
48. Carpenter MH and Kamath H. *Three dimensional extension to the SPARK combustion code* NASA-Langley, 1988, NASA-CP-5029: 107–137.

49. Javed A, Paul PJ, Rajan NKS, et al. Exploration of supersonic confined mixing layer: effect of dissimilar gases at different temperatures. *Proc IMechE Part G: J Aerospace Engineering* 2014; 228: 2255–2265.
50. Javed A, Rajan NKS and Chakraborty D. Effect of side confining walls on the growth rate of compressible mixing layers. *Comput Fluids* 2013; 86: 500–509.
51. Kral LD. Recent experience with different turbulence models applied to the calculation of flow over aircraft components. *Prog Aerospace Sci* 1998; 34: 481–541.
52. Viegas JR and Rubesin MW. *A comparative study of several compressibility corrections to turbulence models applied to high speed shear layers*, 1991, AIAA paper No. 91-1783.
53. Mahle I, Foysi H, Sarkar S, et al. On the turbulence structure in inert and reacting compressible mixing layers. *J Fluid Mech* 2007; 593: 171–180.

Appendix 1

Notations

k	turbulent kinetic energy
u	axial component of velocity
x	axial distance
y	lateral distance
δ'_c	compressible mixing layer growth rate
δ'_{inc}	incompressible mixing layer growth rate
ε	rate of dissipation of turbulent kinetic energy